Newfoundland Labrador

Natural Resources

Mines

TILL GEOCHEMISTRY OF THE TOPSAILS AND RAINY LAKE (NTS MAP AREAS 12H/02 AND 12A/14) AND SURROUNDING AREAS

J.S. Organ and S.D. Amor

Open File NFLD/3301

St. John's
Newfoundland and Labrador
October, 2017

NOTE

DISCLAIMER

Recommended citation:
Organ, J.S. and Amor, S.D.
2017: Till geochemistry of the Topsails and Rainy Lake (NTS map areas 12H/02 and 12A/14) and surrounding areas. Government of Newfoundland and Labrador, Department of Natural Resources, Geological Survey, Open File NFLD/3301, 36 pages.

Cover: Looking northeast from Gaff Topsail to Main Topsail.

Newfoundland Labrador

Natural Resources

Mines

TILL GEOCHEMISTRY OF THE TOPSAILS AND RAINY LAKE (NTS MAP AREAS 12H/02 AND 12A/14) AND SURROUNDING AREAS

J.S. Organ and S.D. Amor

Open File NFLD/3301

GEOLOGICAL SURVEY NEWFOUNDLAND AND LABRADOR 1864

St. John's
Newfoundland and Labrador
October, 2017

CONTENTS

Page

FIGURES

PLATES

ABSTRACT

Analytical results for 499 routine <180μ till samples from north-central Newfoundland, NTS map areas 12H/02, 12A/14 and parts of NTS 12H/03 and 12A/13) are released. These samples have been analyzed by ICP-OES and INAA and checked for acceptable accuracy and precision. The surficial geology is described; however, no interpretation or plotting of the geochemical data have been carried out.

INTRODUCTION

This report complements the release of analytical data for 499 <180μ (–80 mesh) till samples collected over the following NTS map areas: The Topsails (NTS 12H/02); Rainy Lake (NTS 12A/14) and Deer Lake (NTS 12H/03). Three samples were also collected in the southwestern corner of NTS 12A/13 (Corner Brook). Table 1 lists the sample totals for each map area.

Table 1. Samples by NTS map area

NTS Map Area	Map Sheet Name	Number of Routine Till Sample Sites
12A/13	Corner Brook	3
12A/14	Rainy Lake	160
12H/02	Topsails	254
12H/03	Deer Lake	82

The samples were collected during the 2015 field season as part of an ongoing till-geochemistry and surficial mapping program over the island of Newfoundland. The field program also included the determination of the paleo ice-flow history to aid in the subsequent interpretation of geochemical anomalies and understanding of the regional ice-flow history. The work was conducted using truck and ATV traverses, as well as with helicopter support.

Using aerial photography, and ground-truthed data from 546 sites, a map of surficial geology and landforms will be released at a later date, at a scale of 1:50 000, along with an interpretation of the geochemical data.

From the Trans-Canada highway, access to the Topsails *via* the T'Railway (old railway bed) is gained either *via* Route 401 to Howley, or by travelling south on the Buchans Highway (Route 370), turning right at kilometre 14 and continuing on the forest-resource road to Millertown Junction. In the southeastern part of NTS map area 12H/03, access is restricted to a small portion of the T'Railway and a number of forest-resource roads that also provide access to NTS 12A/14 (Figure 1).

BEDROCK GEOLOGY AND MINERAL RESOURCES

The study area lies within the Notre Dame Subzone of the Dunnage Zone of the Newfoundland Appalachians. The Dunnage Zone represents the remnants of the opening and closing of the Iapetus Ocean; it includes volcanic and sedimentary rocks formed in back-arc and island-arc environments, and by post-accretion sedimentary deposition during the Silurian and Devonian periods (O'Reilly *et al.*, 2010). Two groups of predominately granitoid rocks underlie the plateau known as the Topsails. Ordovician gneissic granodiorite, tonalite and minor gabbro make up an older suite of rocks that underlie the western and eastern flanks of the plateau (Taylor *et al.*, 1980); these are intruded by the Silurian (~429 Ma) Topsails Intrusive Suite, consisting of metaluminous and peralkaline granites. The Hinds Lowlands are underlain by the pink, K-feldspar-porphyritic Hinds Brook Granite (Whalen and Currie, 1988; GSNL, 2017a). The western part of the Topsails, west of Hinds Lake, is made up of Silurian (429 Ma) volcanic rocks of the Springdale Group, and Ordovician intrusive rocks of the Rainy Lake Complex (438 Ma), intrud-

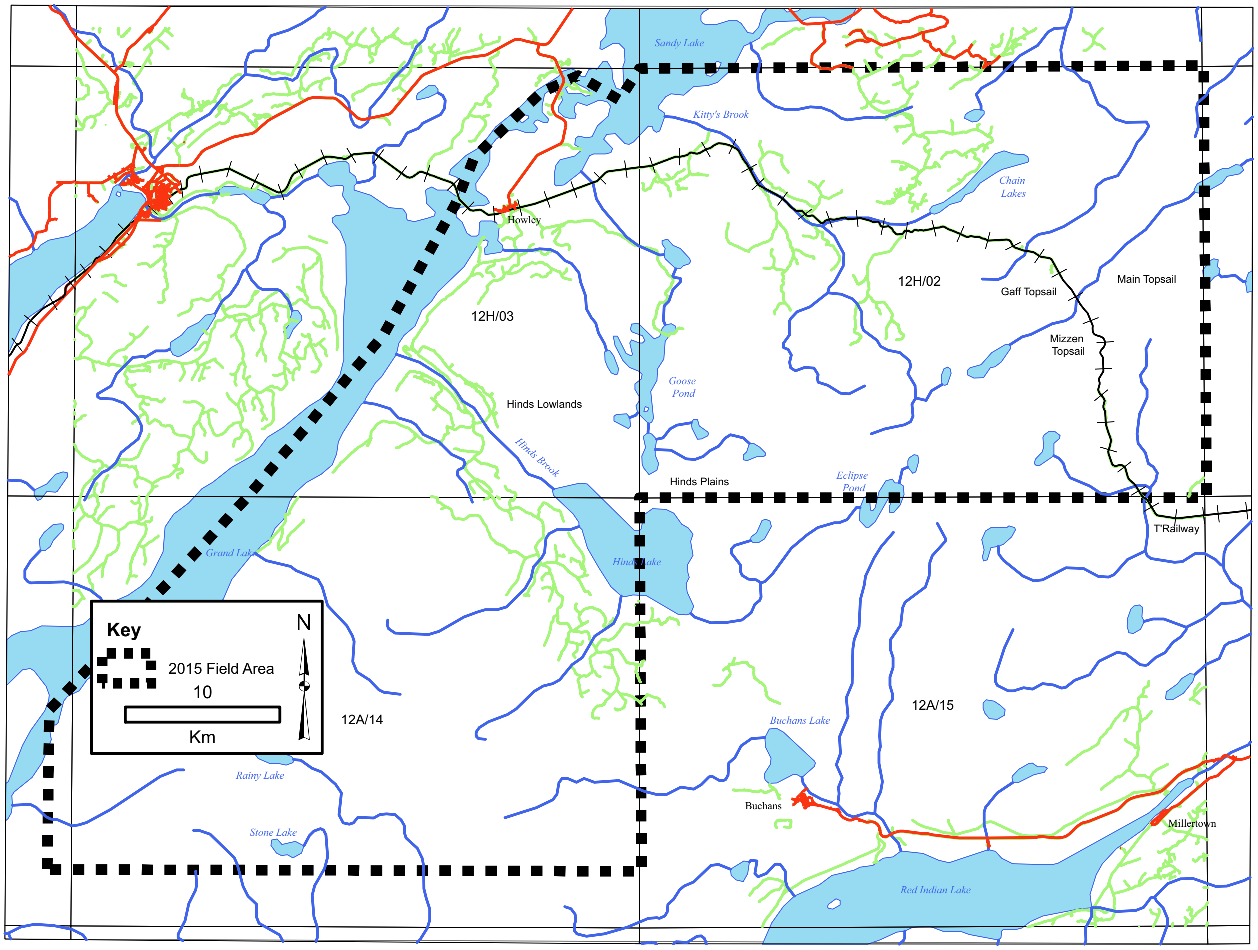

Figure 1. *Location of study area. The boundary of the study area is indicated by the black dotted line. Red lines represent provincial roads; green lines represent forestry-resource roads.*

ed by the Topsails Intrusive Suite (Whalen and Currie, 1988). Carboniferous clastic sedimentary rocks skirt the south edge of Grand Lake and are more abundant on the south shore of Sandy Lake (Whalen and Currie, 1988). The geology of the study area is shown, along with mineral occurrences and till sample locations, in Figure 2.

The first exploitation of resources within the study area was for dimension stone, during the construction of the Newfoundland Railway in 1898. Several granite quarries were in operation during this time, and the granite used for the construction of bridge abutments (for the railway) and for the Railway Station in St. John's (Martin, 1983). Following completion of the railway, these quarries remained inactive for most of the 19th century up until the closure of the Newfoundland Railway in the late 1980s (Kerr, 1994). Increased demand for dimension stone, and improved access to the area, led to staking and exploration, and the opening of the Summit Quarry by Classic Stone Inc. (Kerr, 1994). In 2007, Altius Minerals Inc. and JNR Resources staked a large portion of the study area to investigate its potential for volcanic–hosted uranium (O'Reilly *et al.*, 2010). In addition to uranium, the goals of subsequent exploration programs included the following up of additional indications of copper and molybdenum mineralization (O'Reilly *et al.*, 2010).

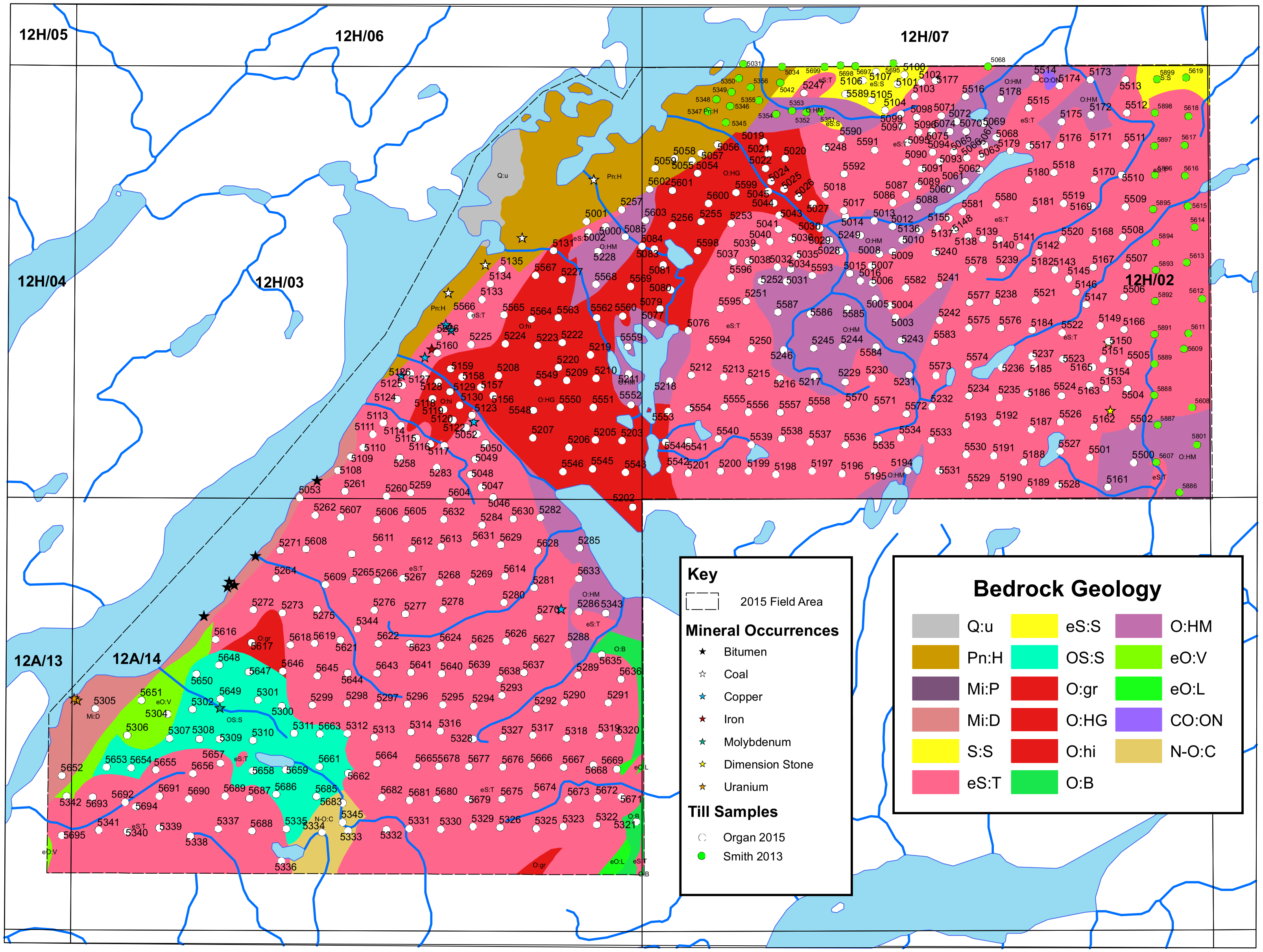

Figure 2. *Caption and legend see page 4.*

Legend

Post-Ordovician Units (Overlap Sequences)

Pleistocene

Q:u **Surficial deposits:** Unconsolidated sediments

Pennsylvanian

Pn:H **Howley Formation:** Grey to red sandstone, pebble-cobble conglomerate and siltstone

Mississippian

Mi:D **Deer Lake Group:** Red and grey conglomerate, sandstone, siltstone and mudstone; grey calcareous dolostone and dolomitic limestone

Early to Late Silurian

S:S **Springdale Group:** Mafic flows and pyroclastic rocks; red sandstone, conglomerate and shale

Post-Ordovician Units (Intrusive Rocks)

Early Silurian

eS:T **Topsails Igneous Suite:** Granite, granodiorite, syenite and gabbro

eS:S **Sheffield Lake Complex:** Variably welded, fine-grained ash-flow tuffs

Late Ordovician to Early Silurian

OS:S **Southern Long Range mafic intrusions:** Mafic plutons, layered gabbro, hornblende gabbro, lecogabbro, diorite, quartz diorite, and minor granodiorite

Iapetus Ocean

(Dunnage Zone (Notre Dame Subzone))

Middle to Late Ordovician

O:gr Massive to moderately foliated granodiorite and minor tonalite

Early to Late Ordovician

O:hi Pink, fine-to medium-grained, biotite+/- muscovite granite and aplite

O:HG **Hinds Brook Granite:** White to pink, medium- to coarse-grained, biotite-amphibole K-feldspar-porphyritic two-

Early to Middle Ordovician

O:B **Buchans Group:** Mafic, intermediate and felsic submarine flows and pyroclastic rocks

O:HM **Hungry Mountain Complex:** Tonalite, granodiorite, diorite,

Early Ordovician

eO:L **Star Lake ophiolite complex:** Local pods and dykes of pegmatitic hornblende diorite and fine-grained hornblende

eO:V **Glover Formation:** Mafic and silicic volcanic rock and high level intrusions with minor volcaniclastic sedimentary rock

Late Cambrian to Early Ordovician

CO:ON **Unnamed ophiolite (Notre Dame Subzone):** Ultramafic rocks, gabbro, trondhjemite, diabase, volcanic and

Neoproterozoic to Early Ordovician

N-O:C **Caribou Lake gneiss complex:** Biotite-muscovite, migmatitic paragneiss and granodioritic to quartz monzonitic

Figure 2. *Sample locations and bedrock geology of the study area (GSNL, 2017a). Samples collected during the 2015 field season are shown as white dots, and those collected prior to 2015 are shown as green dots (Organ, 2014). The locations of mineral showings and indications are identified by stars (GSNL, 2017b).*

Mineral occurrences currently known within the study area comprise past producers of coal (3), and granite (1), one granite prospect, and showings and indications of bitumen (6), copper (6), uranium (2), iron (1), molybdenum (1) and coal (1) (GSNL, 2017b; Figure 2, Table 2).

QUATERNARY HISTORY

The Newfoundland Ice Cap extended out to the continental shelf during the Late Wisconsinan glacial maximum (Grant, 1989; Shaw *et al.*, 2006). Approximately 13 000 years before present (BP), deglaciation became terrestrially based and the deglacial configuration became irregular and time-transgressive because of ice thickness and topography (Shaw *et al.*, 2006). At 12 000 years BP, ice remained over the Topsails (Shaw *et al.*, 2006; Figure 3). As ice continued to retreat, it disintegrated into a number of small isolated ice caps (Grant, 1974). This model proposes that parts of the Topsails were ice-free, and that ice remained over Hinds Lake and the southern part of the study area, with its centre over Red Indian Lake. Batterson (2003) concluded that late-stage ice remained in the higher elevations on the Topsails during deglaciation on either side of Hinds Lake. Smith (2012) also suggested that late-stage ice caps were located in the high elevations west of Buchans, and north and southwest of Red Indian Lake (Figure 4).

Table 2. Mineral occurrences in the 2015 study area

Map Sheet No.	MODS No.	Latitude (°N) (NAD 1927)	Longitude (°W) (NAD 1927)	Occurrence Name	Status	Commodity
12A/14	Cu 002	48.9366	57.0709	Koorae	Showing	Copper
12A/14	U005	48.8839	57.4984	Grand Pond Point #1	Indication	Uranium
12A/14	U006	48.8830	57.4957	Grand Pond Point #2	Indication	Uranium
12A/14	Btm001	48.9669	57.3396	Little Pond Brook	Indication	Bitumen
12A/14	Btm002	48.9520	57.3628	Grand Lake East #1	Indication	Bitumen
12A/14	Btm003	48.9487	57.3642	Grand Lake East #2	Indication	Bitumen
12A/14	Btm004	48.9502	57.3581	Grand Lake East #3	Indication	Bitumen
12A/14	Btm005	48.9321	57.3846	Grand Lake East #4	Indication	Bitumen
12A/14	Mo001	48.8789	57.3703	Harrys Brook	Indication	Molybdenum
12H/02	Stn001	49.0507	56.5879	Quarry Station	Past Producer (Exhausted)	Granite
12H/02	Stn002	49.0899	56.5889	Summit Quarry	Prospect	Granite
12H/03	Col001	49.1850	57.0427	Goose Brook	Past Producer (Dormant)	Coal
12H/03	Col002	49.1515	57.1056	Kelvin Brook	Showing	Coal
12H/03	Col003	49.1196	57.1708	Aldery Brook	Past Producer (Dormant)	Coal
12H/03	Col004	49.1359	57.1383	Coal Brook Mine	Past Producer (Dormant)	Coal
12H/03	Btm027	49.0108	57.2859	Grindstone Point	Indication	Bitumen
12H/03	Cu001	49.0716	57.2121	Hinds Brook	Showing	Copper
12H/03	Cu002	49.0450	57.1482	Spillway	Showing	Copper
12H/03	Cu003	49.0821	57.1914	Penstock	Indication	Copper
12H/03	Cu004	49.1012	57.1729	Bear Brook #1	Showing	Copper
12H/03	Cu005	49.0980	57.1684	Bear Brook #2	Showing	Copper
12H/03	Fe001	49.0870	57.1853	Hinds Lake Road	Indication	Iron

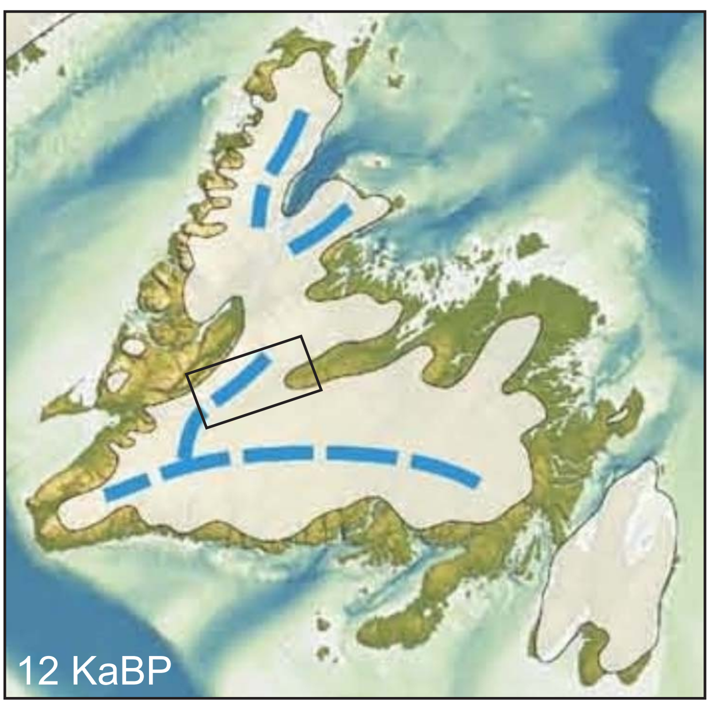

Figure 3. *Pattern of deglaciation on the Island of Newfoundland at 12 000 years BP; blue dashed lines show location of ice divides (Shaw* et al.*, 2006). Black box shows location of study area.*

Impounded water from the retreating Newfoundland Ice Cap formed a long, narrow glacial lake, named glacial Lake Howley, at the present-day location of Grand Lake (Batterson and Catto, 2001; Batterson, 2003). The elevation of an outlet at the southwestern end of glacial Lake Howley controlled the water level, while the opening of topographically lower outlets, as the ice retreated to the northeast, controlled subsequent lowering of the water level of the glacial lake. The lake emptied about 12 300 years BP, based on the elevation of deltas and dating of shells at the head of Deer Lake (Batterson, 2003). Evidence of melting ice and standing water is found along the south shore of Grand Lake, in the form of thick glaciofluvial sediments deposited in a glaciolacustrine environment (Batterson, 2000).

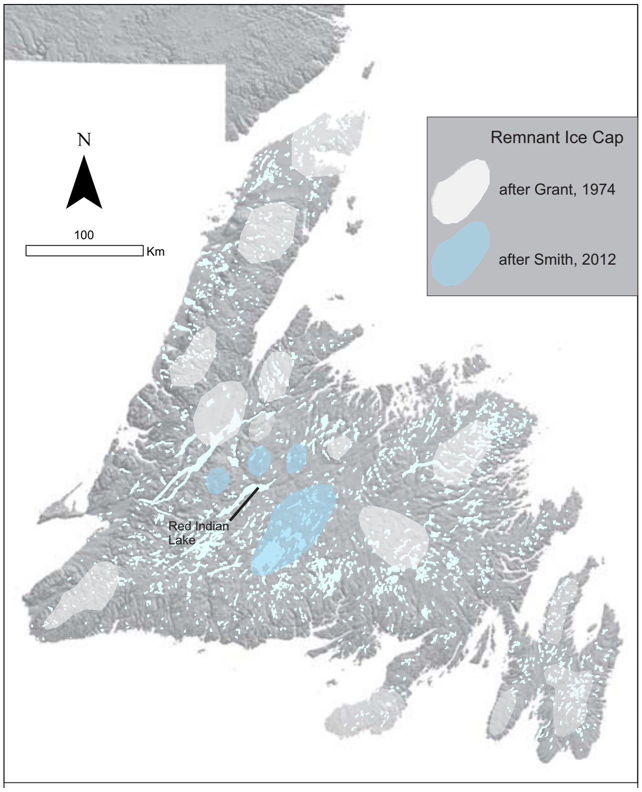

Figure 4. *Map of Newfoundland showing the approximate location of remnant ice caps as the Newfoundland Ice Cap disintegrated, as proposed by Grant (1974). Only those in central Newfoundland, coloured blue, have been modified by Smith (2012).*

Prest *et al.* (1967) first mapped large boulder ridges within the valleys of Kitty's Brook and the Chain Lakes. These ridges, trending southeast to northwest in Chain Lakes, and south to north in Kitty's Brook, are up to 1.6 km long, 9–12 m high, and with crests 90–300 m apart, interpreted as ribbed moraines. During more detailed textural and fabric analyses, Tucker (1974) concluded that the ridges were composed of till, and re-interpreted them as recessional-ablation moraine, deposited during a topographically controlled ice-flow retreat from the valleys onto the Topsails. He also described a small outwash deposit on the north side of Kitty's Brook, that contained both foreset and topset bedding, and interpreted it as a small delta that had formed between the till ridges.

ICE-FLOW HISTORY

Striae indicate that ice flow was radial from an ice-dispersal centre on the Topsails (Taylor and Vatcher, 1993; Batterson, 2003). The flow directions are shown on Figure 5 and have been documented by Vanderveer and Sparkes (1982; southwestward), Taylor and Vatcher (1993; northward), Klassen (1994a; northwestward), Batterson (2003; northwestward and westward), McCuaig *et al.* (2006; westward), Smith (2009; southward), Smith (2010; northward) and Organ (2014; northeastward). Individual striation measurements within the study area are shown in Figure 6. The relationship between the many ice flows remains largely unknown, as only one age relationship has been observed: a northwesterly flow followed by a west-southwesterly flow in Hinds Brook, documented by Batterson (2003). He suggested that an ice-dispersal centre was located on the Topsails with an ice divide along their southwest margin south of Hinds Lake, producing southeasterly and northwesterly flow. However, the relative timing of the radial flow and ice divide, and the relationships between the flows remain unresolved.

SURFICIAL GEOLOGY

Most of the study area is covered by glacial diamicton (till), interspersed with bogs. Glaciofluvial sand and gravel, deposited by flowing glacial meltwater, are located in the Kitty's Brook valley, the south end of Goose Pond, the south side of Grand Lake and in the valleys draining the western part of the Topsails.

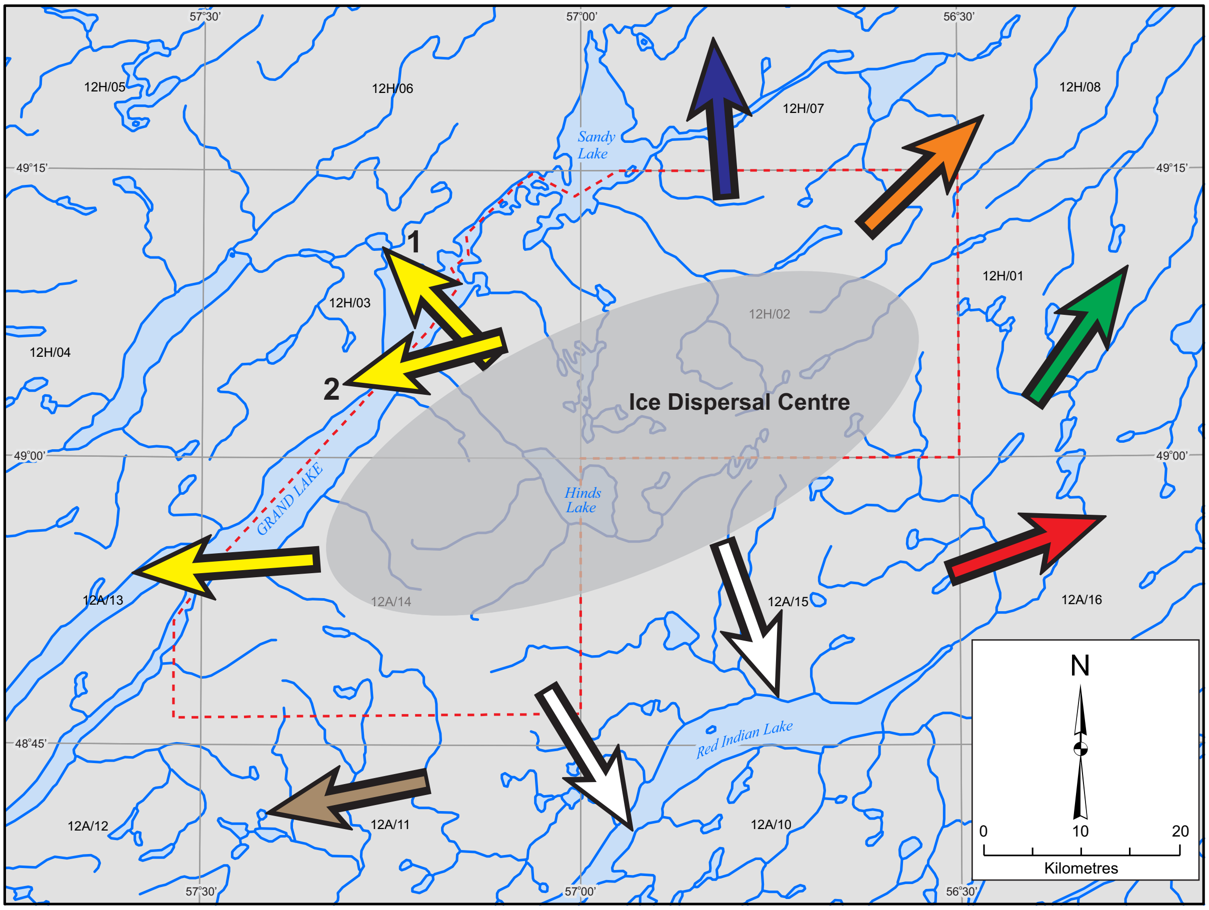

Figure 5. *Regional ice-flow patterns identified within the study area from previous reports by Vanderveer and Sparkes (1982; brown arrow), Taylor and Vatcher (1993; dark blue arrows) Batterson (2003; yellow arrows), Smith (2009; white arrows); Smith (2010; red arrow), Smith (2012; green arrow) and Organ (2014; orange arrow). The only age relationship known is that a northwestward flow (1) is post-dated by a west-southwestward flow (2).*

Relief is high along the southeastern shore of Grand Lake (in NTS map areas 12H/03 and 12A/14), southeast of Sandy Lake (NTS 12H/02) and northeast of Hinds Lake (Lobster House Hill and Hinds Hill); and low west of Goose Pond (NTS 12H/03), southwest of the Topsails centred on Wolf Pond (NTS 12H/02) and east of the Topsails in the southeast corner of NTS 12H/02; relief is moderate elsewhere. The lowest point within the sampled area is the surface of Grand Lake (85 m above sea level), while the highest is Hinds Hill, in the southwest corner of NTS 12H/02, at 667 m. Gaff Topsail, Mizzen Topsail and Main Topsail are 574 m, 544 m and 560 m above sea level (asl) respectively.

GLACIAL DIAMICTON DEPOSITS

Only one stratigraphically continuous unit of glacial diamicton was identified. The diamicton is typically matrix-supported, and ranges from a matrix of silty very fine- to fine-grained sand to one of fine- to medium-grained sand with little silt (Plate 1). The matrix of the diamicton in NTS map area 12H/02 is commonly very compact, and has a clast percentage of about 20% and an

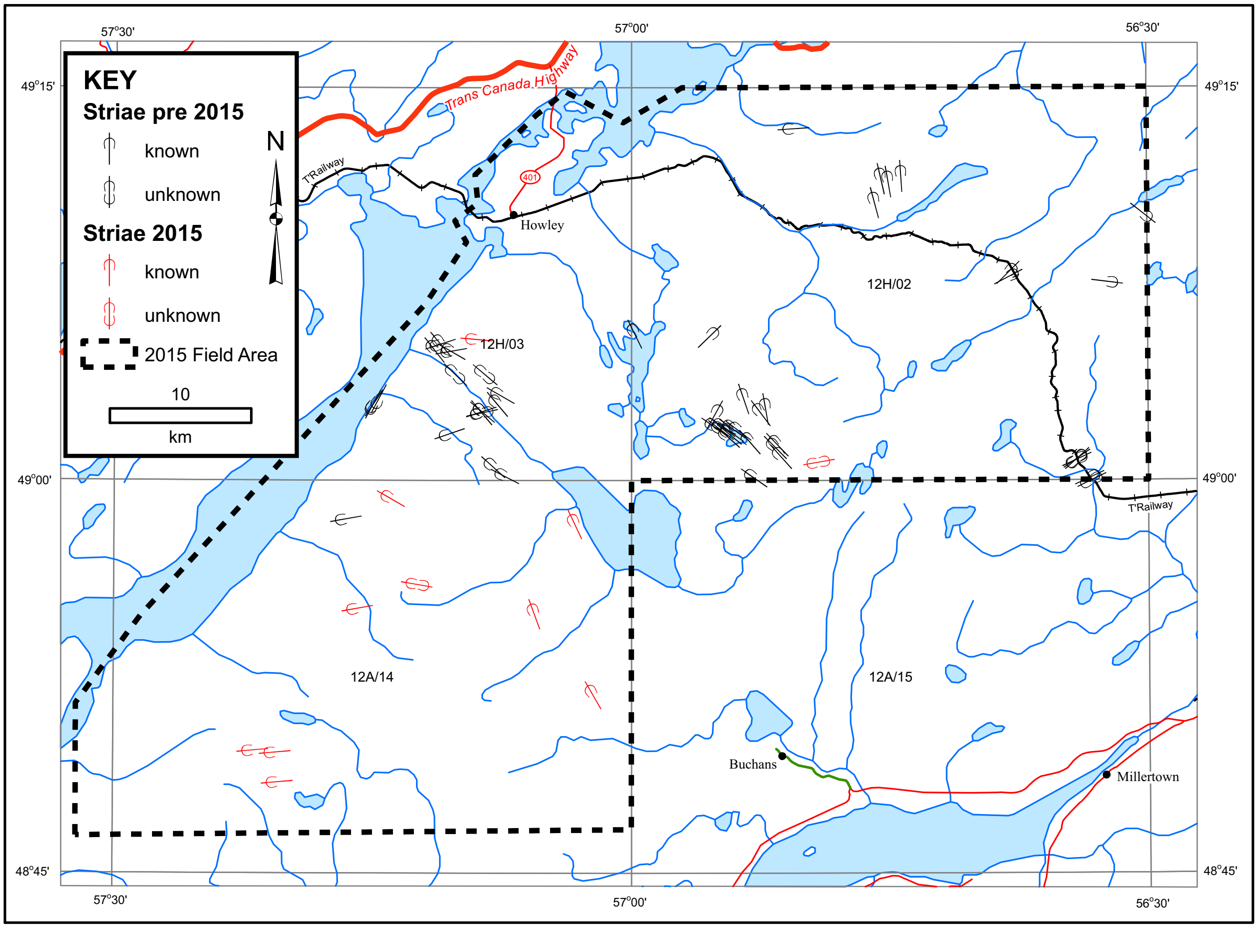

Figure 6. *Locations and orientations of newly identified striae, shown in red, identified during 2015 fieldwork.*

average clast diameter of 3 cm. Striated clasts were observed in only 17%, and faceted clasts in 9% of the 546 sites visited. Clasts encountered on the surface range from pebble to boulder-sized (up to 350 cm diameter). The angularity of the clasts ranges from very angular to subrounded, but is typically subangular. The composition of the clasts reflects that of the local underlying granitic bedrock, and their size and angularity also suggest they have only been transported short distances. The characteristics described above *(i.e.*, compactness, striae on clasts, angular clasts and preferentially oriented landforms) indicate that the diamicton was formed by actively retreating ice, and it is therefore interpreted as till.

The morphology and thickness of glacial diamicton are variable. In the east of the study area, in most of NTS map area 12H/02, blanket, plain and hummocky till, interspersed with bog, mask the underlying bedrock. Veneers of till up to 1.5 m thick, associated with concealed and exposed bedrock, are located in the southwestern and northwestern parts of NTS 12H/02, and throughout NTS 12A/14. Northwest–southeast trending ridges of till are located in the Chain Lakes area in the northern half of NTS 12H/02. Eroded till is characterized by being devoid of fines, and meltwater channels have been cut into thick till north of Hinds Lake and on the western half of NTS 12A/14.

Plate 1. *Till plain with granitic boulders on the surface. Inset shows a typical glacial diamicton within a hand-dug test pit..*

Blankets and plains composed of till are common on the Topsails, while thinner veneers are prevalent west of Hinds Lake. Northwest–southeast trending till ridges are located along Chain Lakes; their orientation changes to north–south at the southern end of the lakes. These are flat-topped, and are up to 2.6 km long and 500 m wide (Plate 2). Tucker (1974) provides detailed descriptions of the till ridges.

Hummocky till is common both southeast and northeast of Chain Lakes (Plate 3). Within areas of hummocky till, the till matrix is sandier (fine- to medium-grained sand and little silt) than that described above. The surface of the hummocks shows a high concentration of angular–sub-angular cobbles and boulders with diameters in excess of 200 cm. The sandiness of the matrix material (suggesting winnowing of fines by melting glacial water) and the high concentration of angular cobbles in the upper part of this unit (resulting from disintegration of ice and subsequent transport of ice-marginal material) suggest that it was formed by stagnating ice under a passive margin. Therefore, the hummocky till is interpreted as a recessional-ablation till. Similar areas of stagnating ice are believed to have been present to the east and northeast of Sheffield Lake (Organ, 2014) and to the south in the Meelpaeg Lake area (Smith, 2010). This is consistent with Grant's (1974) proposed remnant ice cap over the Sheffield Lake area.

Areas where the upper surface of the till has been modified, or cut into, are mapped as eroded till. In some areas, the upper 50 cm of material is devoid of silt and very fine sand, suggesting that it has been washed. Areas of eroded till within the study area are often associated with large

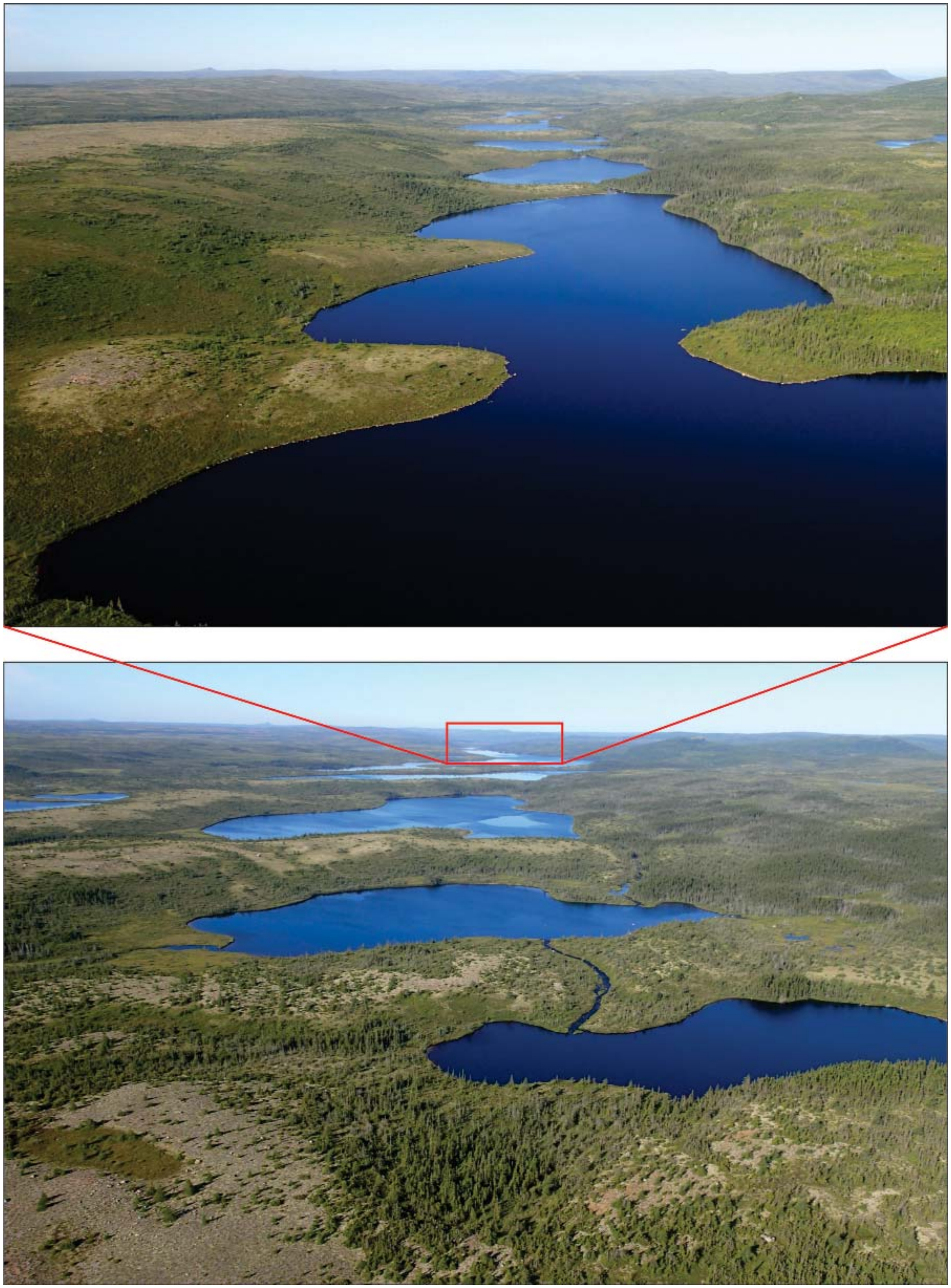

Plate 2. *Lower picture shows northeastern extent of Chain Lakes, looking southwestward towards flat-topped till ridges. Inset from lower picture, shown above, shows till ridges at the southwestern extent of Chain Lakes.*

Plate 3. *Boulder-covered hummocky terrain to the east of Gaff Topsail.*

meltwater channels (Plate 4) or local armouring of the surface with boulders (Plate 5). The channels are up to 10 km long, 250 m wide and 10 m deep; they are believed to have been carved by meltwater produced during the late stages of deglaciation. Batterson (2003) interprets these channels as ice-marginal or proglacial, depending on the orientation of the channel with respect to the slope. The armouring boulders are the result of meltwater removing fines during unchannellized, meltwater sheet flow (Benn and Evans, 1998).

Overall, the tills are much sandier than those described by Smith (2010) to the south, and those to the east described by Organ (2014). The sandy nature of their matrix is believed to be related to underlying granitic bedrock and its mode of erosion, as well as the short transportation distance (Batterson, 2003).

GLACIOFLUVIAL DEPOSITS

Glaciofluvial sands and gravel are located along Kitty's Brook, on the west side of Goose Pond, on the south shore of Grand Lake and in the bottoms of waterways draining the western part of the Topsails. These deposits consist of moderately sorted medium- to coarse-grained sand, and poorly sorted pebble to cobble gravels (Plate 6). These characteristics are consistent with deposi-

Plate 4. *Meltwater channels in NTS map area 12A/14. Lateral channels drained water from right to left, while the channel on the right is perpendicular to the slope and drained towards viewer.*

Plate 5. *Meltwater channels in NTS map area 12A/14. Lateral channels drained water from right to left, while the channel on the right is perpendicular to the slope and drained towards viewer.*

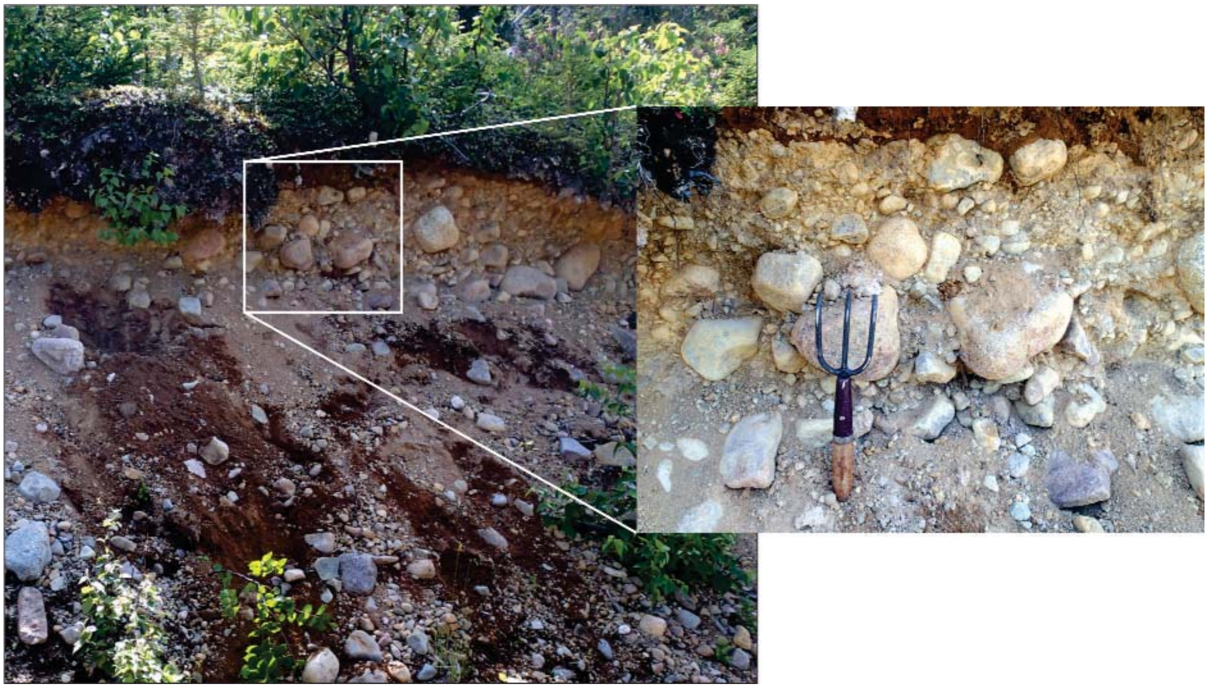

Plate 6. *Pebble- to cobble gravels on the south side of Kitty's Brook.*

tion in meltwater streams that have variable discharge rates. Glaciofluvial sediments range from thin veneers (<1 m) to accumulations tens of metres thick near Howley.

In NTS map area 12H/03, Batterson (2000) identified thick accumulations of glaciofluvial sediment below 170 m asl and interpreted these sediments as having been carried by glacial meltwater from the retreating ice front, and subsequently deposited in glacial Lake Howley. Tucker (1974) identified foreset and topset bedding in sand and gravel on the north side of Kitty's Brook, and interpreted the sand and gravel deposit as a delta formed in a small glacial lake. At the time of Tucker's description, the glaciofluvial material was being exploited in a borrow pit; it was not possible to locate the pit during the 2015 field season.

ORGANIC DEPOSITS

Organic deposits (forming bogs) are found throughout the study area and are most prevalent in the Topsails and Hinds Lake Lowlands, where they are interspersed with till deposits (Plate 7). Typically, these organic deposits are less than a metre thick; however, thicker deposits are present locally.

GLACIAL RETREAT

Field investigations suggest that the pattern of retreat on the Topsails is radial, and late-stage remnant ice remained on the higher elevations east and west of Hinds Lake. This is consistent with retreat patterns observed during previous research in the Grand Lake area (Batterson, 2003), the Red Indian Lake Basin (Smith, 2012), the Chain Lakes (Tucker, 1974), and the Buchans area

Plate 7. *Looking north towards Gaff Topsail in NTS map area 12H/02. Till forms blankets and plain deposits, interspersed with bogs.*

(Klassen, 1994a). The boulder-rich hummocky terrain to the southeast of Chain Lakes suggests that ice stagnated on the Topsails. In the Buchans area, Klassen (1994a) and Batterson (2003) indicated that retreat was to the east and west of Buchans and Hinds Lake. The location of remnant ice on the highlands on either side of Hinds Lake has not been defined and will be the focus of air-photo analysis. No radiocarbon dates are available for the study area; however, Batterson (2003) suggests that deglaciation probably occurred sometime after the opening of the Grand Lake Basin, and the formation of glacial Lake Howley, after 12 600 years BP.

REGIONAL SURFICIAL SEDIMENT SAMPLING

SAMPLING AND SAMPLE PREPARATION METHOD

Till sampling for geochemical analysis was completed in NTS map area 12H/02 and covered 90% of NTS 12A/14 (north of 48°47'N), and NTS 12H/03 southeast of Grand Lake (about 30% of the area of that map area). Three samples were also collected in the southeast corner of NTS 12A/13 (Figure 2).

Approximately 1 kg of till was collected, and placed in a Kraft paper bag, from the C- or BC-soil horizons exposed in 358 hand-dug pits (median sample depth 55 cm), 69 roadcuts (median sample depth 80 cm), 44 ditches (median sample depth 73 cm), 22 mudboils (median sample depth 40 cm), two river sections (median sample depth 93 cm), two trenches (median sample depth 70 cm) and two pits or quarries (median sample depth 40 cm). Sample spacing was determined by access along existing roadways and the availability of appropriate sample material. Along forest-resource and other roads, the sample density was one sample every 1 linear kilometre whereas in remote areas, only accessible via helicopter, it decreased to one sample per 4 km^2. Field-duplicate samples were collected at 44 sites, resulting in an overall frequency of 1 in 12, to estimate the natural inhomogeneity of the sample medium. The results of the field-duplicate analyses are summarized in a later section.

A total of 543 samples (including the 44 field duplicates) were submitted to the Geochemical Laboratory of the GSNL where they were air-dried in ovens at 60°C and dry-sieved to <180 µm (-80 mesh) in stainless steel sieves. An additional 49 samples were collected in 2013 in the northwest corner and 26 in the eastern one-tenth of NTS 12H/02 (Organ, 2014). Nine samples were also collected by Klassen (1994b) in the southeastern corner of NTS 12H/02. The locations of these samples are shown in Figure 2; however, their analyses will be released in a separate report (Organ and Amor, 2017).

ANALYSIS

The <180 µ fraction was subjected to inductively-coupled plasma optical emission spectrometry (ICP-OES) analysis after multi-acid ($HF/HCl/HNO_3/HClO_4$) digestion, and instrumental neutron-activation analysis (INAA) at Becquerel Labs (now known as Maxxam Analytics) in Mississauga, Ontario. Of the 49 elements determined, 12 were determined by both ICP-OES and INAA (As, Ba, Ce, Co, Cr, Fe, La, Mo, Na, Rb, Sc and Zr). Loss-on-ignition (LOI) was determined gravimetrically. A complete list of analytical variables is given in Table 3, and the analytical methods are described in detail in Appendix A.

Analyses of 499 till samples (excluding field duplicates) are presented as part of this report as a comma-delimited ASCII attachment in Appendix B, where the analytical variables are labelled with a combination of the element name, a numeric code denoting the analytical method, and the unit of measurement. Analyses of 12 samples were conducted in 2017, as opposed to 2016, due to having been overlooked previously.

QUALITY ASSURANCE

Quality assurance in the lab consisted of insertion of one certified reference standard (TILL-1, TILL-2, TILL-3 or TILL-4; Lynch, 1996), and one analytical duplicate in every sequence of 20 samples. Standard analyses for both analytical methods, in 2016 and 2017, and duplicate analyses for INAA and ICP-OES were satisfactory and no re-analyses were necessary. Control charts are included as Appendix C.

ACCURACY

Comparison of the standard analyses with 'recommended values' for ICP-OES (based on the arithmetic means of multiple re-analyses, prior to the release of the certified material) indicate that the multi-acid digestion is near total (>95% recovery) for Ba, Ca, Co, Fe, K, Li, Mg, Mn, Na, Ni, P, Rb, Sc, Sr and V, and only partial (< 75%) for Be, Y and Zr (Table 4). The greatest underesti-

Table 3. Geochemical variables with analytical method, units, detection limit and number of analyses below the detection limit; one sample was only analyzed for INAA elements and LOI and one sample was only analyzed for LOI

Element	Method	Units	D.L.	<D.L.	Element	Method	Units	D.L.	<D.L.
Ag	AAS	ppm	0.1	485	**Mg**	ICP-OES	%	0.01	0
Al	ICP-OES	%	0.01	0	**Mn**	ICP-OES	ppm	1	0
As	INAA	ppm	0.5	22	**Mo**	INAA	ppm	1	439
As	ICP-OES	ppm	2	105	**Mo**	ICP-OES	ppm	1	254
Au	INAA	ppb	1	477	**Na**	INAA	%	0.1	1
Ba	INAA	ppm	50	2	**Na**	ICP-OES	%	0.01	0
Ba	ICP-OES	ppm	1	0	**Nb**	ICP-OES	ppm	1	5
Be	ICP-OES	ppm	0.1	0	**Ni**	ICP-OES	ppm	1	0
Br	INAA	ppm	1	4	**P**	ICP-OES	ppm	1	0
Ca	ICP-OES	%	0.01	0	**Pb**	ICP-OES	ppm	1	17
Cd	ICP-OES	ppm	0.1	77	**Rb**	INAA	ppm	5	3
Ce	INAA	ppm	3	0	**Rb**	ICP-OES	ppm	1	0
Ce	ICP-OES	ppm	1	0	**Sb**	INAA	ppm	0.1	44
Co	INAA	ppm	2	116	**Sc**	INAA	ppm	0.1	0
Co	ICP-OES	ppm	1	0	**Sc**	ICP-OES	ppm	0.1	0
Cr	INAA	ppm	10	69	**Se**	INAA	ppm	1	496
Cr	ICP-OES	ppm	1	0	**Sm**	INAA	ppm	0.1	0
Cs	INAA	ppm	0.5	35	**Sr**	ICP-OES	ppm	1	0
Cu	ICP-OES	ppm	1	5	**Ta**	INAA	ppm	0.2	4
Dy	ICP-OES	ppm	0.1	0	**Tb**	INAA	ppm	0.5	4
Eu	INAA	ppm	0.5	10	**Th**	INAA	ppm	0.4	1
Fe	INAA	%	0.1	0	**Ti**	ICP-OES	ppm	1	0
Fe	ICP-OES	%	0.01	0	**U**	INAA	ppm	0.1	0
Hf	INAA	ppm	1	0	**V**	ICP-OES	ppm	1	0
K	ICP-OES	%	0.01	0	**W**	INAA	ppm	1	455
La	INAA	ppm	1	0	**Y**	ICP-OES	ppm	1	0
La	ICP-OES	ppm	1	0	**Yb**	INAA	ppm	0.5	0
Li	ICP-OES	ppm	0.1	1	**Zn**	ICP-OES	ppm	1	0
LOI	Gravimetric	%	0.1	0	**Zr**	INAA	ppm	100	5
Lu	INAA	ppm	0.05	0	**Zr**	ICP-OES	ppm	1	0

mation is for Zr (20% of the recommended values). For several elements, the recovery is greater than 100%, indicating that the element is being overestimated; the greatest overestimation is for Sr (average 117% of the recommended values). Overall, ten elements (Ba, Ca, Fe, K, Li, Mg, Mn, Na, P and Rb) out of 29 show recoveries within ±5% of 100%.

Not surprisingly, near-total analyses by INAA are more numerous, because they are not dependent on mineral solubility in a digestion reagent. Recoveries of 95% or less were only reported for Br, Co, Hf, La, Lu, Tb, U, Yb and Zr (Table 5). Fifteen elements out of 26 (As, Ba,

Table 4. Accuracy of ICP-OES analyses

	Till-1	Till-2	Till-3	Till-4	Average
Al	0.94	0.95	0.96	0.96	95%
As	0.93	0.98	0.93	0.94	94%
Ba	0.93	0.98	0.99	0.98	97%
Be	0.55	0.76	0.58	0.74	66%
Ca	0.94	0.97	0.96	0.98	96%
Ce	0.91	0.85	0.94	0.87	89%
Co	1.08	1.14	1.10	1.16	112%
Cr	0.94	0.95	0.92	0.87	92%
Cu	0.87	0.90	0.89	0.91	89%
Fe	0.98	1.00	1.00	1.00	100%
K	1.03	0.93	0.94	0.93	96%
La	0.93	0.89	0.92	0.92	92%
Li	0.96	0.96	0.99	0.95	96%
Mg	0.97	0.99	0.98	0.96	97%
Mn	1.00	1.03	1.01	1.05	102%
Mo	0.59	0.97		0.95	84%
Na	1.04	1.06	1.04	1.03	104%
Nb	0.82	0.80	0.85	0.90	84%
Ni	1.03	1.11	1.05	1.25	111%
P	0.90	0.96	1.01	1.0	97%
Pb	0.68	0.77	0.74	0.87	76%
Rb	1.02	1.01	1.01	1.03	102%
Sc	1.14	1.12	1.10	1.17	113%
Sr	1.13	1.18	1.15	1.22	117%
Ti	0.82	0.87	0.95	0.94	89%
V	1.03	1.07	1.06	1.05	105%
Y	0.69	0.45	0.75	0.49	59%
Zn	0.91	0.93	0.93	0.96	93%
Zr	0.15	0.20	0.27	0.18	20%

Calculated as the arithmetic mean of multiple analyses of each certified reference standard, divided by the recommended value for the standard.

Table 5. Accuracy of INAA analyses

	Till-1	Till-2	Till-3	Till-4	Average
As	0.98	0.98	1.00	1.00	99%
Au	1.61	1.13	0.75	0.93	111%
Ba	1.00	0.95	0.99	0.96	98%
Br	0.97	0.96	0.78	0.85	89%
Ce	0.99	1.02	0.96	1.04	100%
Co	0.94	1.08	0.88	0.79	92%
Cr	0.98	0.95	0.94	1.04	97%
Cs	0.99	0.99	1.11	1.06	104%
Eu	1.22	1.08			115%
Fe	1.00	0.97	0.96	1.00	98%
Hf	1.0	0.93	0.730	1.15	95%
La	0.95	0.98	0.86	1.01	95%
Lu	0.93	0.99	0.91	0.92	94%
Mo				1.07	107%
Na	1.00	0.99	0.96	1.02	99%
Rb	1.00	0.98	1.01	1.0	100%
Sb	0.97	1.00	0.94	0.98	97%
Sc	1.08	1.01	0.94	1.10	103%
Sm	1.06	1.03	1.07	1.07	106%
Ta	1.12	1.05	0.75	1.0	98%
Tb	0.88	0.89	0.45	0.86	77%
Th	0.99	0.97	1.03	0.96	99%
U	0.92	0.94	0.95	0.93	94%
W		0.98			98%
Yb	0.84	0.67	0.73	0.66	72%
Zr	0.93	0.85	0.98	0.90	91%

Calculated as the arithmetic mean of multiple analyses of each certified reference standard, divided by the recommended value for the standard.

Ce, Cr, Cs, Fe, Hf, La, Na, Rb, Sb, Sc, Ta, Th and W) show average recoveries within ±5% of 100%, although W is only detectable in one standard (TILL-2).

FIELD AND ANALYTICAL VARIABILITY

The overall precision of the field and analytical duplicates is shown in Table 6. This single parameter does not take into account the variability of precision with concentration levels.

Table 6. Overall analytical and field precision (±% at 95% confidence level)

	Precision			Precision	
Element	**Analytical**	**Field**	**Element**	**Analytical**	**Field**
Al2	2.2	7.9	**Lu1**	21.6	32.8
As1	68.8	109.4	**Mg2**	4.0	27.0
As2	67.8	74.4	**Mn2**	3.7	22.8
Au1	188.9	160.7	**Mo2**	68.5	71.1
Ba1	7.3	23.9	**Na1**	14.4	13.4
Ba2	5.2	20.4	**Na2**	4.3	10.5
Be2	6.7	15.0	**Nb2**	8.1	22.5
Br1	16.0	90.9	**Ni2**	10.7	18.1
Ca2	3.2	22.5	**P2**	4.4	52.8
Cd2	15.6	25.3	**Pb2**	12.7	39.6
Ce1	17.5	26.5	**Rb1**	10.5	25.2
Ce2	6.3	19.6	**Rb2**	5.4	14.6
Co1	91.7	78.3	**Sb1**	52.0	66.7
Co2	4.2	37.7	**Sc1**	14.1	19.0
Cr1	75.0	83.6	**Sc2**	3.7	18.3
Cr2	8.2	22.7	**Sm1**	6.8	16.7
Cs1	52.8	82.4	**Sr2**	4.0	27.3
Cu2	20.4	50.1	**Ta1**	14.2	25.0
Dy2	7.7	17.1	**Tb1**	17.3	30.0
Eu1	40.2	42.8	**Th1**	17.7	14.8
Fe1	12.3	14.6	**Ti2**	6.1	16.6
Fe2	5.2	8.6	**U1**	8.6	18.9
Hf1	12.1	35.2	**V2**	3.6	23.6
K2	2.4	8.1	**Y2**	6.9	16.7
La1	13.0	19.8	**Yb1**	18.6	31.6
La2	6.8	18.9	**Zn2**	4.7	20.0
Li2	5.2	27.2	**Zr1**	26.1	35.7
LOI	3.6	26.7	**Zr2**	8.5	28.6

Therefore, results of analytical and field duplicates for all elements are displayed graphically as plots devised by Thompson and Howarth (1978) in Appendix D. Figures 7 and 8 show examples where elements' repeatability in field duplicates varies significantly from the repeatability in analytical duplicates (Mg by ICP-OES), and where it does not (Ce by INAA). Figure 9 summarizes the precision of all of the analytical parameters, in field and analytical parameters, in bar-chart form.

DISPLAY OF GEOCHEMICAL DATA

The purpose of this report is the timely release of till-geochemical data. No geochemical maps are presented. Geochemical data can be found in Appendix B.

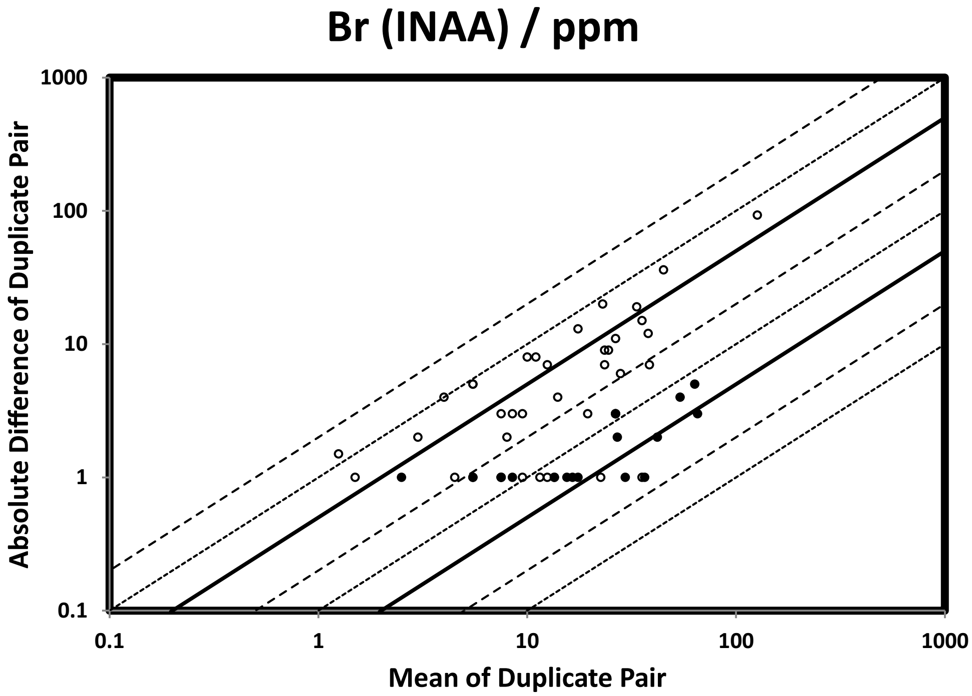

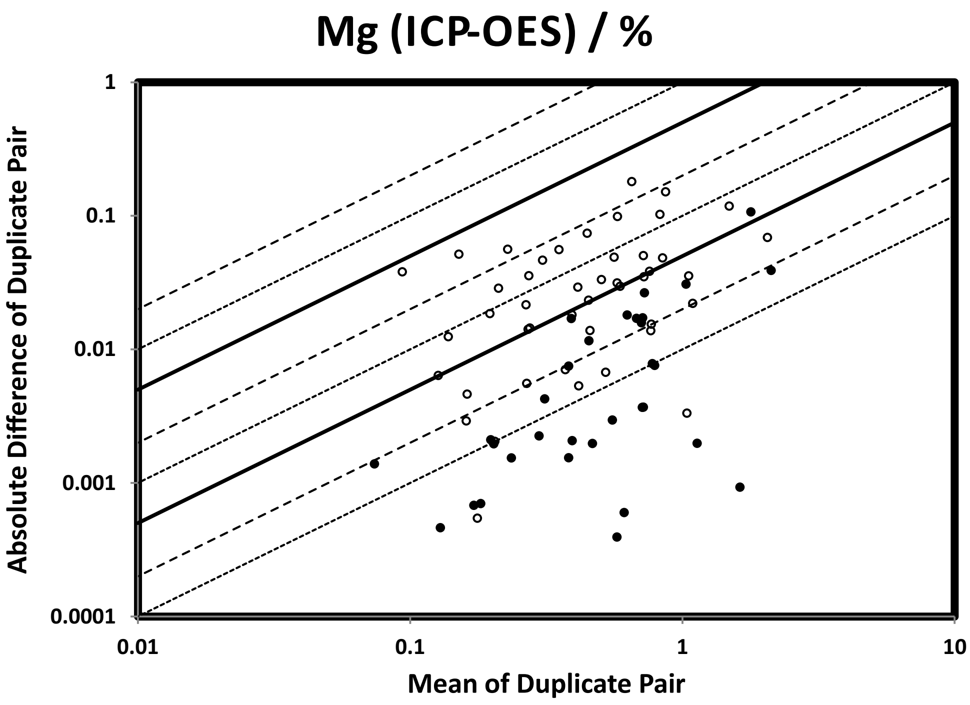

Figure 7. *Thompson-Howarth precision plots for field and analytical duplicates of Br (INAA analyses) and Mg (ICP-OES analyses): examples of elements whose field variability significantly exceeds its analytical variability. In these precision plots, the mean of each pair of duplicates is plotted against their absolute difference; both axes are scaled logarithmically. A series of parallel lines indicates precision of gradually increasing absolute value, from ±1% to ±200%. Field duplicates are denoted by open circles, and analytical duplicates by closed circles; the absolute value of the precision for the former is invariably greater (*i.e.*, the repeatability is worse).*

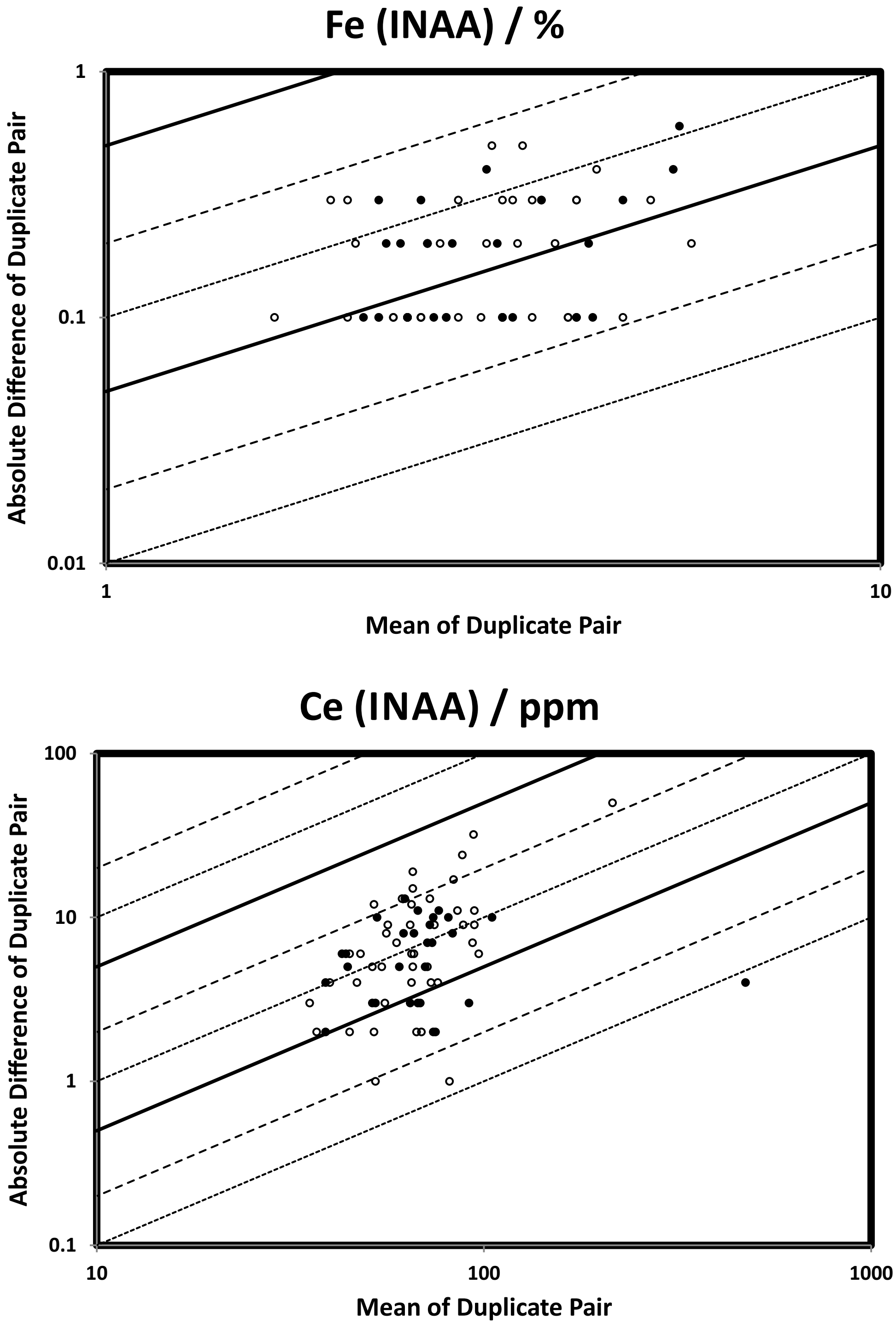

Figure 8. *Thompson-Howarth precision plots for field and analytical duplicates of Fe (INAA analyses) and Ce (INAA analyses): examples of elements whose field variability does not significantly exceed its analytical variability.*

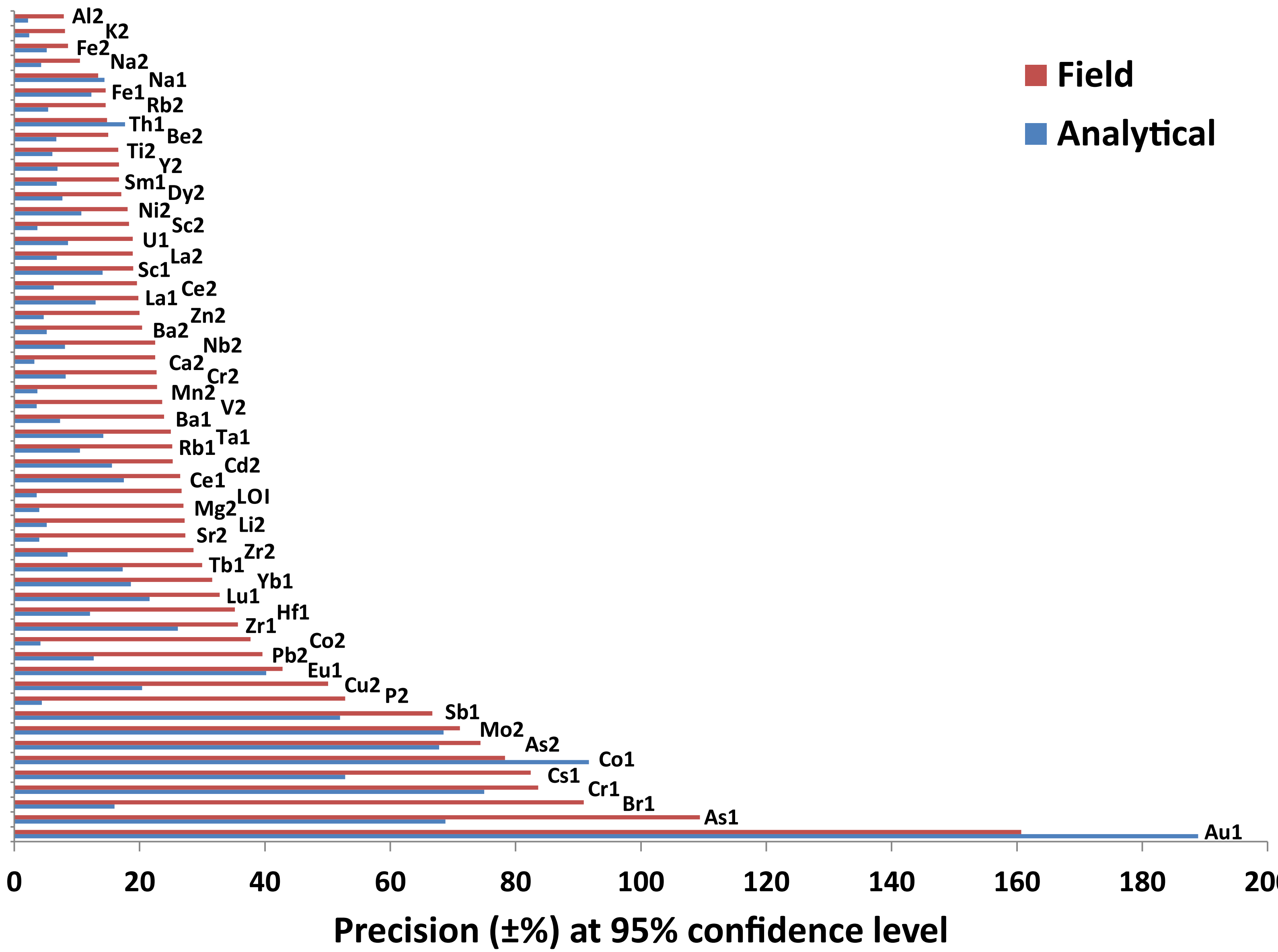

Figure 9. *Bar chart summarizing precision of field and analytical duplicates.*

SUMMARY

During the 2015 surficial mapping field season, 543 till samples (499 routine samples plus 44 field duplicates) were collected in NTS map areas 12H/02 and 12A/14, and parts of 12H/03 and 12A/13. These samples have been analyzed by ICP-OES and INAA and checked for acceptable accuracy and precision.

ACKNOWLEDGMENTS

An early version of this report was reviewed by Sarah Hashmi. The maps were drafted by Terry Sears.

REFERENCES

Batterson, M.J.

2000: Landforms and surficial geology of the Deer Lake map sheet (NTS12H/03). Government of Newfoundland and Labrador, Department of Mines and Energy, Geological Survey, Map 2000-14, Open File, 012H/03/1488.

2003: Quaternary geography and sedimentology of the Humber River basin and adjacent areas. Government of Newfoundland and Labrador, Department of Mines and Energy, Geological Survey, Report 03-02, 194 pages.

Batterson, M.J. and Catto, N.R.

2001: Topographically-controlled deglacial history of the Humber River Basin, western Newfoundland. Geographie physique et Quaternaire, Volume 55, Number 3, pages 213-228.

Benn, D.L. and Evans, D.J.A.

1998: Glaciers and glaciation. Arnold Publishers, Great Britain, 734 pages.

Finch, C.J.

1998: Inductively coupled plasma-emission spectrometry (ICP-ES) at the Geochemical Laboratory. *In* Current Research. Government of Newfoundland and Labrador, Department of Mines and Energy, Geological Survey, Report 98-1, pages 179-193.

Geological Survey of Newfoundland and Labrador

2017a: "Generalized Bedrock Geology." Newfoundland and Labrador GeoScience Atlas OnLine. Last update: January 2013. http://geoatlas.gov.nl.ca/ . [March 2017]"

2017b: "Mineral Occurrence Database System (MODS)." Newfoundland and Labrador GeoScience Atlas OnLine. Last update: April 12, 2017. http://geoatlas.gov.nl.ca/. [April 2017].

Grant, D.R.

1974: Prospecting in Newfoundland and the theory of multiple shrinking ice caps. *In* Report of Activities. Geological Survey of Canada, Paper 74-1B, pages 215-216.

1989: Quaternary geology of the Atlantic Appalachian region of Canada. *In* Quaternary Geology of Canada and Greenland. *Edited by* R.J. Fulton. Geological Survey of Canada, Geology of Canada, Paper 76-1A, pages 283-285.

Kerr, A.
1994: Magmatic, hydrothermal and surficial processes in the development of multicoloured dimension stone granites of the Topsails Plateau area (NTS 12H/2). *In* Current Research. Government of Newfoundland and Labrador, Department of Mines and Energy, Geological Survey, Report 94-1, pages 147-165.

Klassen, R.A.
1994a: A preliminary interpretation of glacial history derived from glacial striation, central Newfoundland. *In* Current Research, Part D. Geological Survey of Canada, Paper 94-1D, pages 117-143.

1994b: Till geochemistry and ice flow data Central Newfoundland (NTS 12A/10, 12A/15, 12A16 and 12H/1). Geological Survey of Canada, GSC Open File 2823, 338 pages.

Lichte, F.E., Golightly, D.W. and Lamothe, P.J.
1987: Inductively coupled Plasma-Atomic emission Spectrometry. *In* Methods for Geochemical Analysis. U.S. Geological Survey Bulletin 1770, pages B1-B10.

Lynch, J.
1996: Provisional elemental values for four new geochemical soil and till reference materials, TILL-1, TILL-2, TILL-3 and TILL-4. Geostandards Newsletter, Volume 20, Number 2, pages 277-287.

McCuaig, S.J., Liverman, D.G.E. and Taylor, D.M.
2006: Till geochemistry of the Glover Group, western Newfoundland (NTS map areas 12A/12 and 12A/13). Government of Newfoundland and Labrador, Department of Natural Resources, Geological Survey, Open File 12A/1209, 84 pages.

Martin, W.
1983: Once upon a mine: The history of pre-confederation mining in Newfoundland. Canadian Institute of Mining and Metallurgy, Special Volume, 26, 102 pages.

Organ, J.S.
2014: Springdale-Sheffield Lake surficial ice-flow mapping results with potential implications for glacial lake Howley. *In* Current Research. Government of Newfoundland and Labrador, Department of Natural Resources, Geological Survey, Report 14-1, pages 231-248.

Organ, J.S. and Amor, S.
2017: Till geochemistry of Sheffield Lake, Springdale, Gull Pond and The Topsails (NTS map areas 12H/07, 08, 01, 02). Government of Newfoundland and Labrador, Department of Natural Resources, Open File 012H/2212, 40 pages.

O'Reilly, D., Devereaux, A., Courage, D., Winter, L., Churchill, R., Annesley, I.R. and Bradley, K.
2010: First and second year assessment report on geological, geochemical and trenching exploration for licences 16779M, 16829M-16830M, 16832M, 16836M-16837M, 16842M, 16848M, 16854M and 16858M-16867M on claims in The Topsails area, west-central Newfoundland. JNR Resources Incorporated and Altius Resources Incorporated. Newfoundland and Labrador Geological Survey, Assessment File NFLD/3148, 390 pages.

Prest, V.K., Grant, D.R. and Rampton, V.N.
1967: Glacial Map of Canada, Geological Survey of Canada Map 1253A.

Shaw, J., Piper, D.J.W., Fader, G.B., King, E.L., Todd, B.J., Bell, T., Batterson, M.J. and Liverman, D.G.E.
2006: A conceptual model of the deglaciation of Atlantic Canada. Quaternary Science Reviews, Volume 25, pages 2059-2081.

Smith, J.S.
2009: Red Indian Lake project: A review of Quaternary Investigations southeast of Red Indian Lake, Newfoundland. *In* Current Research. Government of Newfoundland and Labrador, Department of Natural Resources, Geological Survey, Report 09-01, pages 339-356.

2010: Glacial stratigraphy of the southwest Red Indian Lake Basin, Newfoundland: Preliminary results. *In* Current Research. Government of Newfoundland and Labrador, Department of Natural Resources, Geological Survey, Report 10-01, pages 201-217.

2012: The paleogeography of glacial Lake Shanadithit, Red Indian Lake basin, Newfoundland: Implications for drift prospecting. *In* Current Research. Government of Newfoundland and Labrador, Department of Natural Resources, Geological Survey, Report 12-01, pages 207-227.

Taylor, D.M.
2001: Newfoundland and Labrador striation database. Newfoundland and Labrador Geological Survey, Open File NFLD/2195, Version 4.0.

Taylor, D.M. and Vatcher, S.
1993: Late Wisconsinan delgacial ice-flow patterns in west-central Newfoundland. *In* Current Research. Government of Newfoundland and Labrador, Department of Mines and Energy, Geological Survey Branch, Report 93-01, pages 175-179.

Taylor, R.P., Strong, D.F. and Kean, B.F.
1980: The Topsails Igneous Complex: Silurian-Devonian peralkaline magmatism in western Newfoundland. Canadian Journal of Earth Sciences, Volume 17, pages 425-439.

Thompson, M. and Howarth, R.J.
1978: A new approach to the estimation of analytical precision. Journal of Geochemical Exploration, 9(1), pages 23-30.

Tucker, C.M.
1974: Unusual till ridges in the Kitty's Brook Chain Lakes area of west-central Newfoundland. Maritime Sediments, Volume 10, pages 8-13.

Vanderveer, D.G. and Sparkes, B.G.
1982: Regional Quaternary mapping: an aid to mineral exploration in west-central Newfoundland. *In* Prospecting in Areas of Glaciated Terrain – 1982. *Edited by* P.H. Davenport. Canadian Institute of Mining and Metallurgy, Geology Division, pages 284-299.

Whalen, J.B. and Currie, K.L.
1988: Geology, Topsails Igneous Terrane, Newfoundland. Geological Survey of Canada, Map 1680A, Scale 1:200 000.

APPENDIX A: Analytical Methods

Gravimetric Analysis (LOI)

Organic content was estimated from loss-on-ignition (LOI) during a controlled combustion in which 1g aliquots of sample were gradually heated to 500°C in air over a 3 hour period.

Inductively Coupled Plasma-Optical Emission Spectrometry (ICP-OES)

For these analyses, the procedures outlined by Finch (1998) were followed. One gram of sample was weighed into a 125 ml Teflon beaker, and 15 ml HF (~48%), 5 ml of concentrated HCl and 5 ml of 1:1 $HClO_4$ were added to each sample. The samples were placed on a hotplate at 200°C and evaporated to dryness, after which 5 ml concentrated HCl and 45 ml deionized water were added and returned to the hotplate at 100°C. When the residue was completely dissolved the samples were removed, cooled and transferred to 50 ml volumetric flasks. One ml of 50 g/l boric acid was added to each sample to remove any residual hydrofluoric acid. The samples were made up to volume and analyzed by ICP-OES (Lichte *et al.*, 1987). The following elements were determined: Al, Ba, Be, Ca, Ce, Co, Cr, Cu, Dy, Fe, K, La, Li, Mg, Mn, Mo, Na, Nb, Ni, P, Pb, Rb, Sc, Sr, Ti, V, Y, Zn and Zr.

Instrumental Neutron Activation Analysis (INAA)

These analyses were carried out at Becquerel Labs (now known as Maxxam Analytics), Mississauga, Ontario. An average of 24 g of sample was used for analysis and the samples were weighed and encapsulated in the Geochemical Laboratory of the Department of Natural Resources in St. John's. Samples were irradiated with flux wires and an internal standard (1 for 11 samples) at a thermal neutron flux of 7 x 10^{11}n/cm^{2}s. After 7 days (to allow Na^{24} to decay), samples were counted on a high purity Ge detector with a resolution better than 1.7 KeV. Using the flux wires, the decay-corrected activities were compared to a calibration developed from multiple certified international reference materials. The standard present is only a check on accuracy of the analysis and is not used for calibration purposes. Ten to 30 percent of the samples were checked by re-measurement. This method measures the total contents of the following elements: As, Au, Ba, Br, Ce, Co, Cr, Cs, Eu, Fe, Hf, La, Lu, Mo, Na, Rb, Sb, Sc, Se, Sm, Ta, Tb, Th, U, W, Yb and Zr.

Atomic-Absorption Spectrometry (AAS)

0.5 g of sample is weighed into each 10 ml digestion tube. 2 ml of nitric acid are added, and the tubes are capped and left overnight. The next day, the digestion tubes are heated in a digestion block at 90°C for two hours. The tubes are shaken every 30 minutes. When digestion is complete, the samples are cooled and made up to a final volume of 10 ml with distilled deionized water and analyzed for silver by ICP-OES (Lichte, 1987). Only Ag was analyzed by this method.

APPENDIX B:

Digital Data Listing

Suffixes

1: INAA

2: ICP-OES after multiacid ($HF/HCl/HNO_3/HClO_3$) digestion

6: AAS after nitric acid digestion.

The data are available as a digital comma separated file (.csv) through this link.

APPENDIX C:

Control Charts

In each chart, a dashed black line represents the expected value (the mean of multiple analyses, carried out at several labs, and reported by Lynch (1996) and two continuous black lines represent the upper and lower 'limits of acceptability', established by adding and subtracting two standard deviations (also reported by Lynch, *op. cit.*). Charts for certain elements are omitted because the latter were undetectable in the establishment of recommended values.

Suffixes

1: INAA

2: ICP-OES after multiacid ($HF/HCl/HNO_3/HClO_4$) digestion

Units

- Al2, Ca2, Fe1, Fe2, K2, Mg2, Na1, Na2 in weight percent.
- As1, As2, Ba1, Ba2, Be2, Br1, Ce1, Ce2, Co1, Co2, Cr1, Cr2, Cs1, Cu2, Eu1, Hf1, La1, La2, Lu1, Mn2, Li2, Mo1, Mo2, Nb2, Ni2, P2, Pb2, Rb1, Rb2, Sb1, Sc1, Sc2, Sm1, Sr2, Ta1, Tb1, Th1, Ti2, U1, V2, Zn2 and Zr2 in parts per million (ppm).
- Au1 in parts per billion (ppb).

The charts are available as a pdf file through this link.

APPENDIX D:

Thompson-Howarth Precision Plots of Field and Analytical Duplicates

In these precision plots, the mean of each pair of duplicates is plotted against their absolute difference; both axes are scaled logarithmically. A series of parallel lines indicates precision of gradually increasing absolute value, from ±1% to ±200%. Field duplicates are denoted by open circles, and analytical duplicates by closed circles; the absolute value of the precision for the former is invariably greater (*i.e.*, the repeatability is worse).

The plots are available as a pdf file through this link.